

Chapter 8

Skin, Nail, and Hair in Rheumatology

Ximena Wortsman MD

Introduction

Ultrasound has been present in the medical arsenal for more than 70 years. However, in the past 30 years, US took a giant leap as the technique passed from a phase of purely experimental use to a widely available imaging procedure used in standard daily clinical practice. The usage of ultrasound for studying skin started in 1951 with the work of Meyer et al. [1] but has continued its development through the years. In 1979, Alexander and Miller studied the skin using pulsed ultrasound [2]. Later on, during the 1980s and 1990s, several groups started to use compact high-frequency ultrasound machines with fixed-frequency probes that currently can vary from 20 to 100 MHz [3–7]. Due to their high-frequency probes and configuration, these machines present high resolution but low penetration. Though this enables the examiner to detect the dermis and upper hypodermis, they lack color Doppler capabilities which means that they cannot detect blood flow. Nevertheless, they provide valuable information in a bitmap-type image about local skin changes. In the year 2004, the first experience in the use of high- and variable-frequency probes with multichanneled color Doppler machines in dermatologic lesions was reported [8]. Since then, dermatologic applications of ultrasound have been growing rapidly, covering a wide range of common lesions such as benign and malignant skin tumors, vascular anomalies, inflammatory diseases, nail lesions, scalp and hair pathologies, and cosmetic applications, among others [9–11]. However, such imaging technique requires both an appropriate ultrasound machine and an operator trained in dermatologic pathologies. This combination is essential to attain the desired outcomes, as it is the integration of the information generated by the visual inspection of the lesion as well as the anatomical data provided by sonography which would

X. Wortsman (✉)

Departments of Radiology and Dermatology, IDIEP-Institute for Diagnostic and Research of the Skin and Soft Tissue, Clinica Servet, Faculty of Medicine, University of Chile, Santiago, Chile
e-mail: xworts@yahoo.com

enable achieving the assessment targets [12]. The limitations for this type of imaging study are lesions that measure ≤ 0.1 mm, epidermal only lesions and pigments such as melanin [10, 12, 13]. However, having all these settings, ultrasound presents an accuracy of diagnosis up to 97% in common dermatologic entities [13].

Normal Ultrasound Anatomy of the Skin, Nail, and Hair

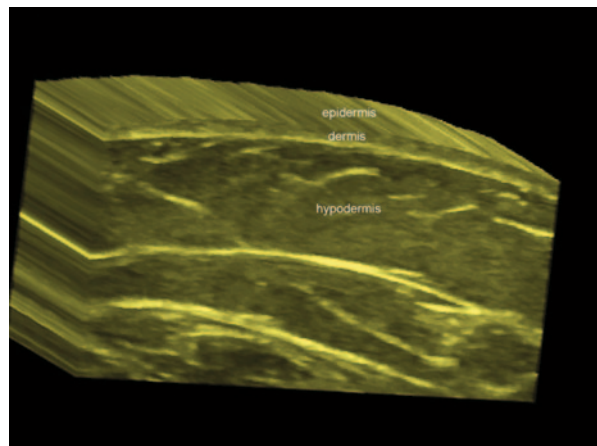
Skin

The epidermis is the most superficial layer of the skin and shows on ultrasound as a hyperechoic layer on non-glabrous skin (i.e., that not from the palms and soles) and as a bilaminar hyperechoic layer in glabrous skin (i.e., that from palms and soles). Its echogenicity is due to the keratin content. The dermis presents as a hyperechoic band, less bright than the epidermis, and its echogenicity is mainly due to the presence of collagen. With age, a hypoechoic band can be observed in the upper dermis. This is called subepidermal low-echogenicity band (SLEB) and corresponds to the deposit of glycosaminoglycans in the skin due to photoaging. The hypodermis appears as a hypoechoic layer due to its fatty lobules that are separated by hyperechoic septa. Slow flow arterial and venous vessels are commonly detected in the hypodermis and occasionally in the dermis ([10, 12–15]; Fig. 8.1).

Nail

This is an enthesis organ that makes up a complex with the interphalangeal joint and the distal insertion of the extensor tendon. The nail unit can be divided in the

Fig. 8.1 Sonographic anatomy of the normal skin (3D reconstruction dorsal forearm, *transverse view*)



ungual and periungual regions. The unguinal region is composed of a hypoechoic nail bed mainly made up of collagen that may turn to slightly hyperechoic in the proximal region where the matrix is located. Above the nail bed, there is a hyperechoic bilaminar structure that is called the nail plate which is composed of hard keratin and has two layers: the dorsal and ventral plates separated by a hypoechoic interplate space. This virtual space turns to hyperechoic on higher frequencies (≥ 20 MHz). Underlying the nail bed, there is a hyperechoic line that corresponds to the bony margin of the distal phalanx. The periungual region is mostly composed of skin without fatty lobules and is divided into the lateral and proximal nail folds. However, hypodermal fatty tissue is prominent in the pulp of the fingers or toes ([16–20]; Fig. 8.2).

Hair

Scalp hair can be divided into two parts: the deep part which is the hair follicle located in the dermis, and the superficial (visible) part that makes up the hair tract. The hair follicle appears on ultrasound as an oblique hypoechoic dermal band and the scalp hair tract mostly shows as a trilaminar hyperechoic structure and $\leq 20\%$ may show a bilaminar hyperechoic pattern. The vellus hair present in the rest of the body appears as a hyperechoic monolaminar structure. The hair follicles can show different depth according to the cycle of the hair, also called the “hair clock hair.” Thus, immature hair follicles (telogen phase) are located in the upper dermis and mature hair follicles (anagen phase) are located in the deep dermis close to the upper hypodermis. In between these phases, there is a catagen phase. Also, the orientation of the hair follicles may present some differences according to ethnic parameters. Hence, hair follicles tend to be more oblique in Caucasians, almost parallel in individuals with African ancestry and more vertical in persons with Asian ancestry. The blood flow of the scalp shows a centripetal pattern and mainly originates from branches of the temporal and occipital arteries. ([21–24]; Figs. 8.3 and 8.4).

Technical Considerations

Ultrasound examinations start with the visual inspection of the lesion and the regulation of the lighting in the examination room in order to assess the presence of single or multiple lesions. A copious amount of gel is applied in the lesional and perilesional region. Comparisons with the contralateral side are also performed. The sonographic test begins with a gray scale sweep that is followed by a color or power Doppler sequence and then the distribution, thickness, type, and speed of the blood vessels is determined by spectral curve analysis. The ultrasound examinations

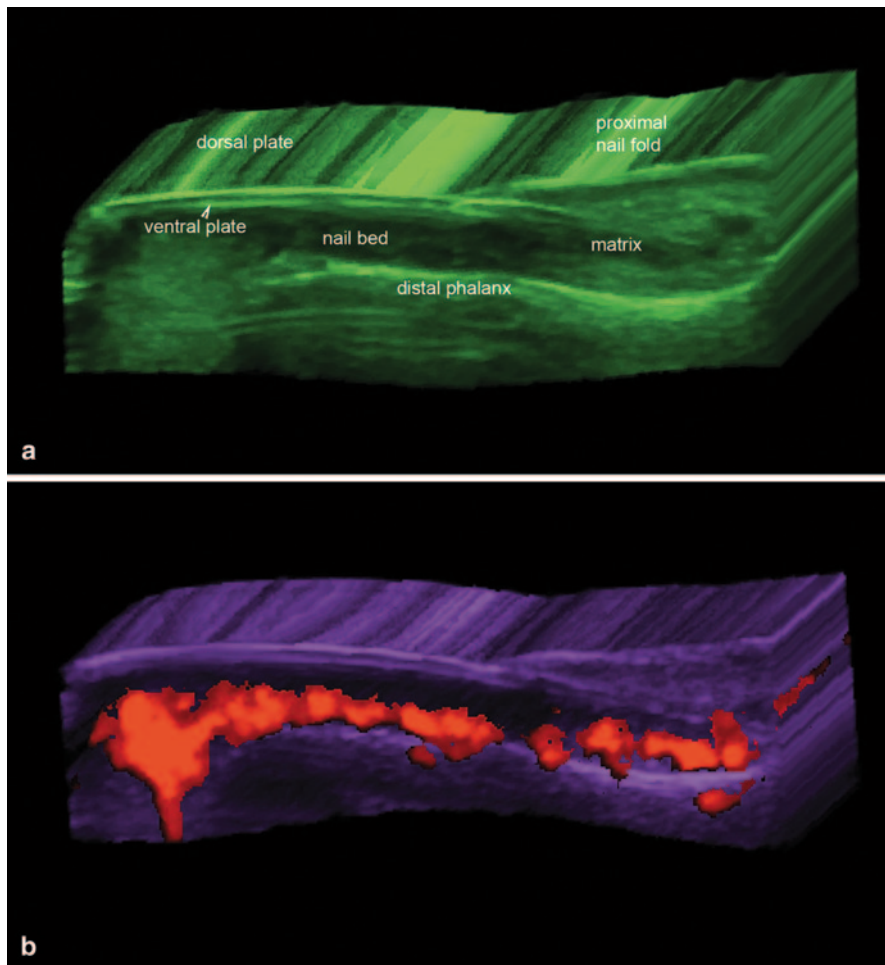


Fig. 8.2 Sonographic anatomy of the normal nail. **a, b** 3D reconstructions (**a**: gray scale and **b**: power Doppler; longitudinal views, index finger; color filter) show the parts of the nail unit (**a**) and the ungual vessels (**b**), in color)

should include at least two sweeps in perpendicular axes (transverse and longitudinal). Frequently, 3D reconstructions are performed in order to clearly demonstrate the pathology to the clinicians. In children ≤ 4 years old, sedation is commonly used in order to avoid movements or crying of the child that can produce artifacts on the screen. Normally, chloral hydrate or melatonin is administered 30 min before the ultrasound examination. The chloral hydrate dosage used is 50 mg/kg and the melatonin dosage varies according to age. Chloral hydrate allows deeper sedation than melatonin; therefore, melatonin is normally not used in periorificial lesions such as around the eyes or mouth because the child can easily wake up. In these

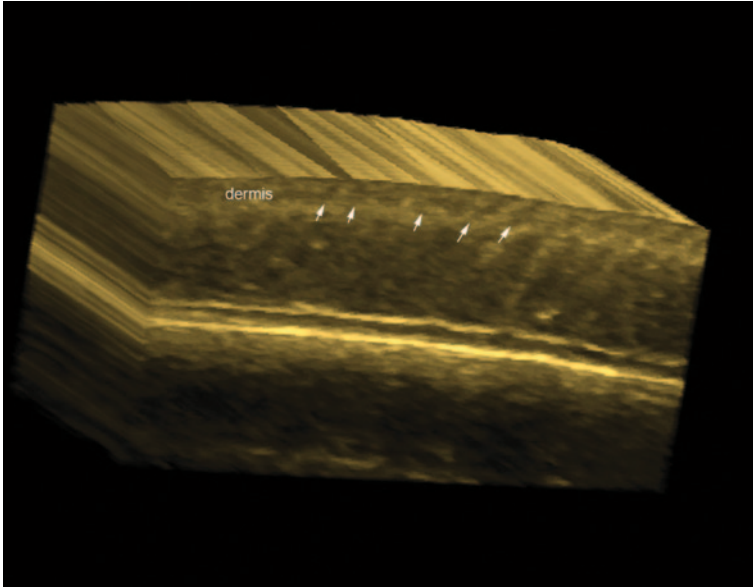


Fig. 8.3 Sonographic anatomy of the normal hair follicles (*arrows*) of the scalp

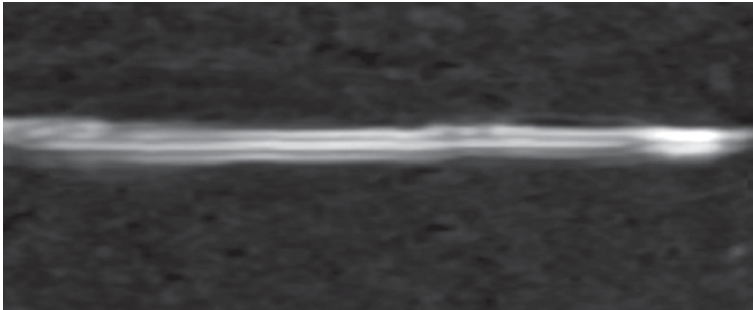


Fig. 8.4 Sonographic anatomy of a normal trilaminar hair tract of the scalp

last cases, the preferred sedative is chloral hydrate. The child is monitored using the modified Aldrete scoring and only discharged when the score is ≥ 9 points [9, 12, 13, 25–27].

Pathologies

There are several dermatologic pathologies that can be scanned on ultrasound. However for academic purposes, we have divided the rheumatologic topics into the following parts:

Inflammatory Diseases

Psoriasis: Skin and Nail Involvement

This is an autoimmune disease that affects the skin, nails, entheses, and joints. The role of ultrasound is to support an early diagnosis and to assess activity and monitoring of the disease [28, 29]. Cutaneous psoriatic plaques appear on ultrasound as thickening and/or undulation of the epidermis with decreased echogenicity and thickening of the upper dermis. Increased blood flow is usually detected in the dermal region of the plaque during active phases. Psoriatic onychopathy presents from early to late phases with thickening (i.e., increased distance between the ventral plate and the bony margin of the distal phalanx) and decreased echogenicity of the nail bed, loss of definition of the ventral plate, hyperechoic deposits in the ventral plate, loss of definition of both plates, wavy and thickened dorsal and ventral plates. Importantly, early changes in psoriatic onychopathy may be subclinical [20]. Commonly, hypervascularity can be detected in the proximal part of the nail bed during the active stages of the disease. Decreased or heterogeneous echogenicity of the tendons (due to enthesopathy), anechoic fluid or hypertrophic synovium in the joints as well as periarticular bony erosions can also be present ([29–35]; Figs. 8.5 and 8.6).

Morphea

This is the cutaneous form of scleroderma, a connective tissue disease, and can show dermal, hypodermal, and fascial involvement. This latter fascial type is also called eosinophilic fasciitis. Morphea can go from inflammatory to atrophic stages and generate multiple plaque-type lesions; affect one or both sides of the body or produce a linear type of involvement which is frequently seen in children and can present as “en coup de sabre” (ECDS), progressive hemifacial atrophy (Parry–Romberg Syndrome, PRS), among other subtypes [34, 36–38]. The phases show different patterns on ultrasound which can be used for assessing the activity of the disease [38]. Usually during the inflammatory phase, there is thickening and decreased echogenicity of the dermis and increased echogenicity of the underlying hypodermis. In the atrophy phase, there is thinning of the dermis and hypodermis, sometimes with absence of fatty lobules, which can generate direct contact between the muscle and the dermis. In between these phases, there is an inactive phase. Frequently, in patients with multiple morphea plaques, there are asynchronous activity between different plaques or parts of the same plaque. This subclinical data could be critical for the early management of these cases [34, 38].

Increased regional blood flow and hyperechogenicity of the hypodermis have been reported as the most sensitive sonographic signs for assessing activity in

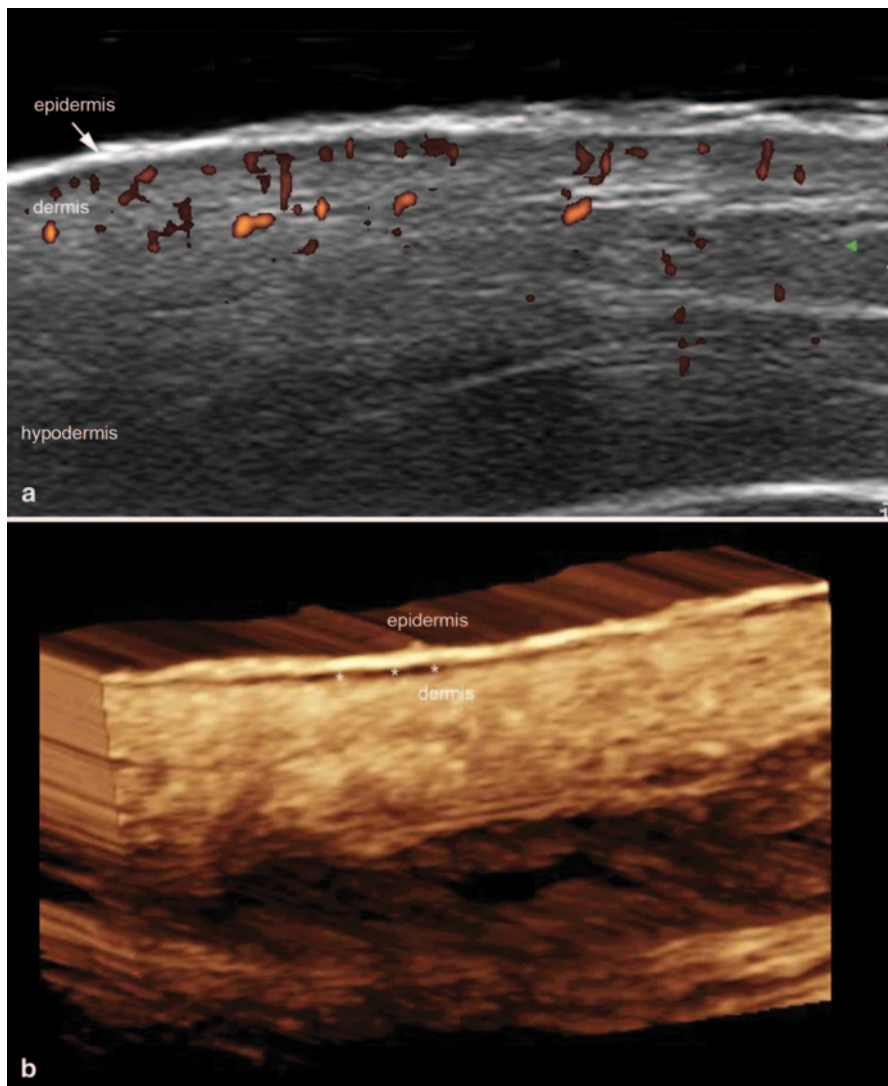
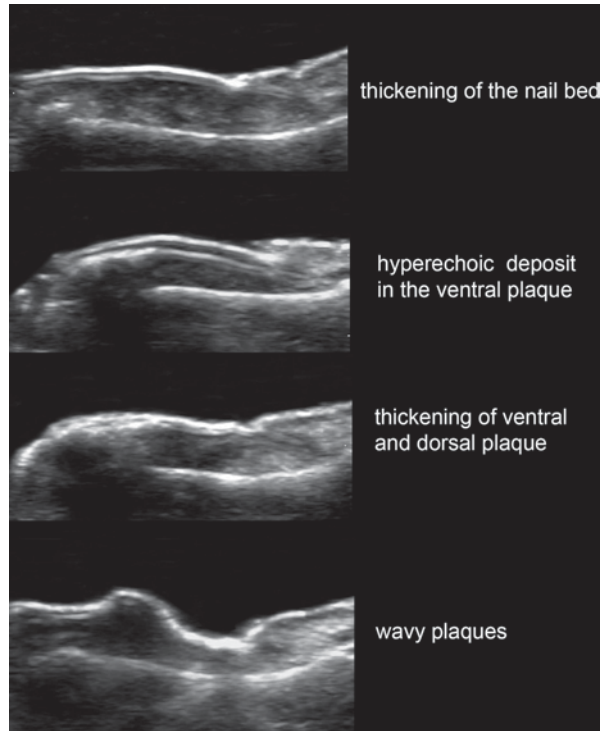


Fig. 8.5 Cutaneous psoriasis plaque. **a** Power Doppler and **b** 3D reconstruction *gray scale*. Notice the thickening of the epidermis and the hypoechoic band in the upper dermis (*). Increased vascularity (**a**, in *color*) is also shown in the dermal part of the plaque (**a**)

morphea. Also, inflammatory signs of the ipsilateral parotid gland (i.e., decreased echogenicity and/or hypervascularity) have been reported in concomitance with Parry–Romberg Syndrome [34, 38]. Upward displacement of the nail plate, increased thickness, and decreased echogenicity of the nail bed due to edema, have also been reported in scleroderma ([20]; Fig. 8.7).

Fig. 8.6 Common sonographic alterations in psoriatic onychopathy



Dermatomyositis

This is an autoimmune disease that affects skeletal muscle, skin, and lungs. On sonography, increased echogenicity of the muscle due to inflammation has been reported. Calcinosis cutis is a common finding in this condition which can be detected on ultrasound as hyperechoic dermal or hypodermal deposits that show a posterior acoustic artifact. These calcinosis deposits may also be seen in the periungual regions at the tip of the fingers. Increased echogenicity of the hypodermis due to panniculitis may also be seen ([20, 34]; Fig. 8.8).

Cutaneous Lupus

This is the cutaneous manifestation of lupus erythematosus which may precede its systemic involvement. According to activity, cutaneous lupus has three phases: acute, subacute, and chronic, also called discoid lupus. On sonography, the acute phase shows as thickening and decreased echogenicity of the dermis with increased echogenicity of the underlying hypodermis and regional hypervascularity (Fig. 8.9). Occasionally, the dermal involvement may take a fusiform shape. In the discoid or chronic lupus, there is atrophy and hypoechogenicity of the dermis with hypovascularity. Isolated increased echogenicity of the hypodermis in the acute phase can also be observed

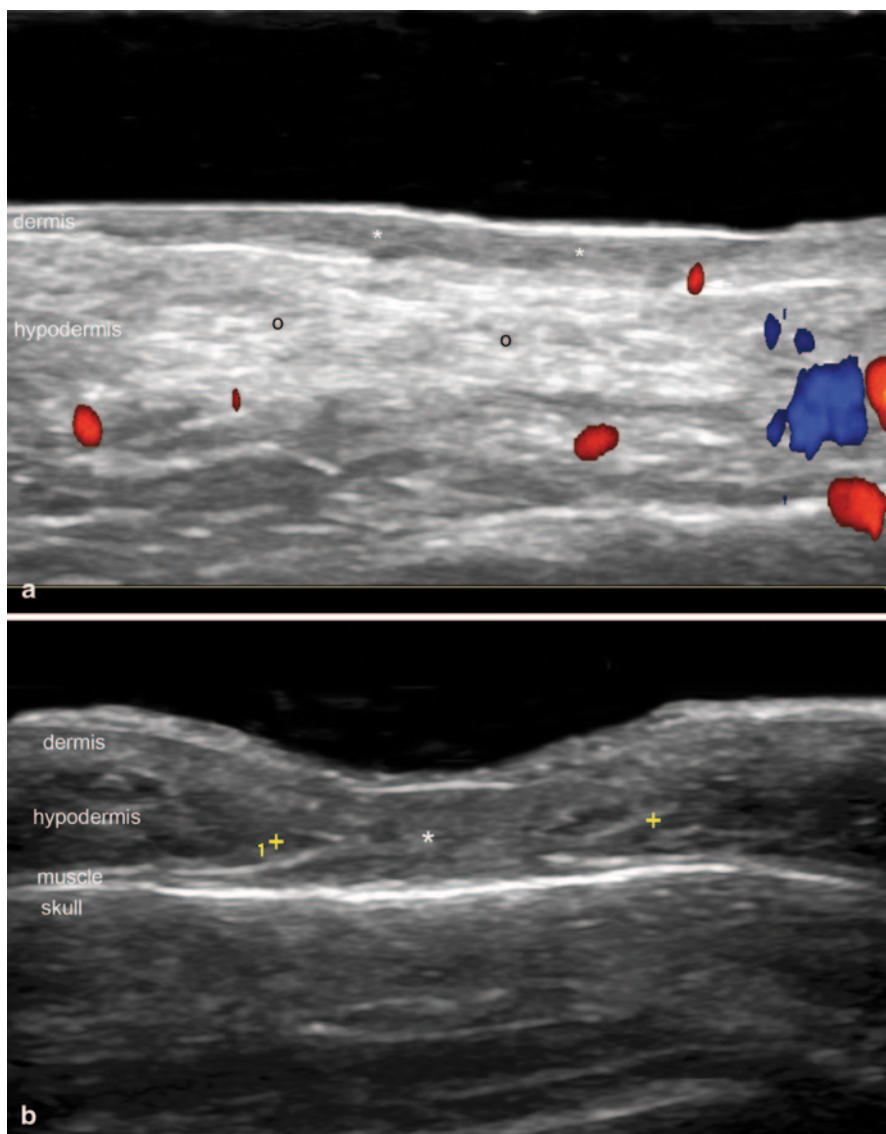
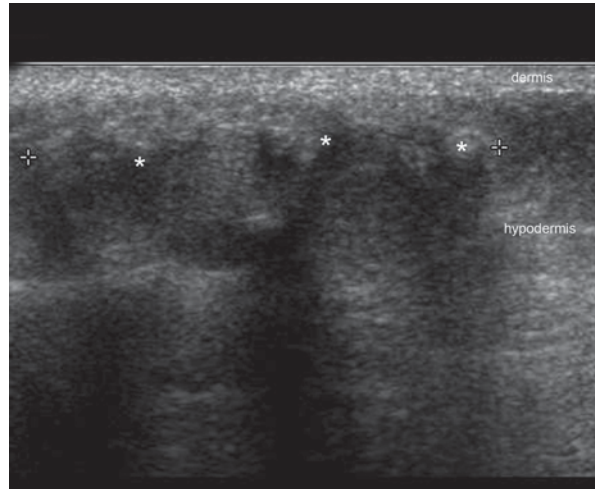


Fig. 8.7 Morphea. **a** Active phase (*color Doppler; transverse view; right cheek*) shows thickening and decreased echogenicity of the dermis (*) with increased echogenicity of the underlying hypodermis (o). A vessel is observed in the dermal part of the lesion (*arrow*). **b** Atrophy phase (*gray scale; frontal region; transverse view*) demonstrates lack of fatty tissue in the hypodermis (*, *between markers*) in the lesional area

which is called “lupus panniculitis” or “lupus profundus.” Additionally, thrombosis and vasculitis may complicate the disease. The thrombosis appears as hypoechoic material within the vessels that show lack of blood flow. The disease may also affect the nail matrix and bed and cause inflammatory and/or atrophic changes in the unguis region with dystrophy (i.e., irregularities) of the nail plate [20, 34].

Fig. 8.8 Dermatomyositis, calcinosis. Ultrasound (*gray scale, transverse view, right gluteal region*) shows hyper-echoic calcified deposits (*, *between markers*) in the hypodermis with posterior acoustic shadowing artifact



Rheumatoid Arthritis

This is a systemic autoimmune inflammatory disease that affects the joints in concomitance with diverse organs which include the nails. Ultrasound may support the early assessment of anatomic changes within the joints such as synovitis, periarticular bony erosions, narrowing of the joint space, tendinopathy, tear or atrophy of the tendons, among other signs. In the nail unit, rheumatoid arthritis produces thickening and decreased echogenicity of the nail bed with regional hypervascularity during the active phases of the disease. Upward displacement of the unguial plaques can also be detected due to edema ([20]; Fig. 8.10). In contrast with psoriatic onychopathy, these patients do not show prominent involvement of the nail plate [35].

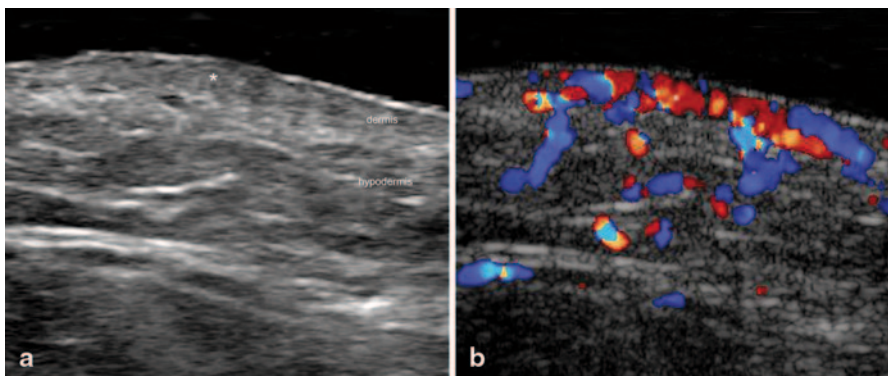


Fig. 8.9 Acute Lupus. **a** Ultrasound (*gray scale, transverse view, right mandible region*) demonstrates thickening and decreased echogenicity of the dermis in the lesional area (*). **b** Color Doppler ultrasound shows increased vascularity in the region (*)

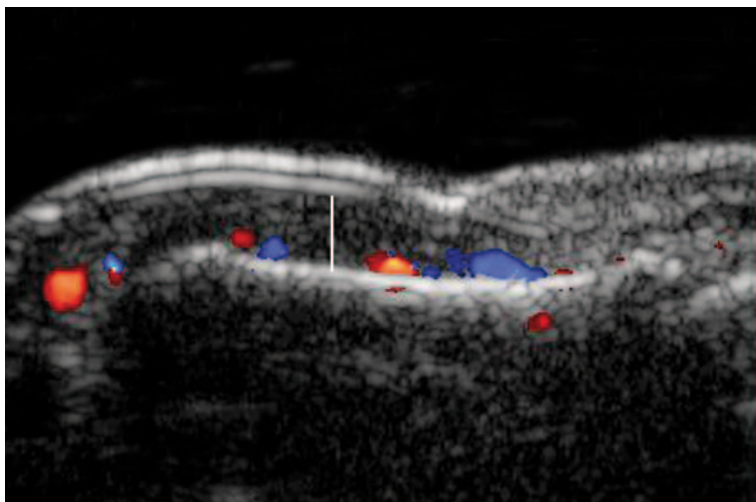


Fig. 8.10 Rheumatoid arthritis. Color Doppler ultrasound of the nail demonstrated upward displacement of the unguis plaques due to thickening of the nail bed (*vertical white line*)

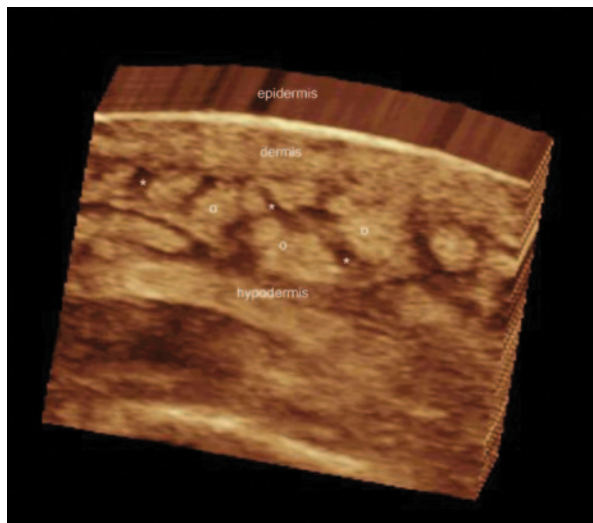
Immunosuppression Complications

Rheumatologic patients are commonly immunosuppressed, which could be related to their primary diseases and/or long-term immunosuppression treatment. Thus, common secondary dermatologic problems may be detected or monitored under sonography [39, 40]. Among these entities are:

Cellulitis or Panniculitis

These are inflammations of the hypodermal layer and could have several origins such as autoimmune issues, trauma, or infection. This inflammatory process usually involves both the lobules and septa; however, it can be divided in lobular or septal panniculitis according to the principal involved part. On sonography, there is increased echogenicity of the hypodermis, commonly with hypervascularity shown on color or power Doppler. However, in the mainly septal forms of panniculitis such as erythema nodosum, there is prominent thickening and hypoechogenicity of the septa. Anechoic fluid or hypoechoic inflammatory interlobular tissue may show a “cobblestone” appearance of the hypodermis ([34]; Fig. 8.11). In the presence of fat necrosis, anechoic pseudocystic structures may be seen due to liquefaction of the fatty tissue [41, 42].

Fig. 8.11 Septal panniculitis with “cobblestone appearance.” 3D reconstruction ultrasound (gray scale, *transverse* view, anterior aspect of the *right* leg) shows increased echogenicity and thickening of the hypodermal fatty lobules (*). Thickening and decreased echogenicity of the hypodermal septa (*) is also noted



Abscesses

These are infectious anechoic or heterogeneous fluid collections normally with echoes due to detritus commonly found in the hypodermis (Fig. 8.12). Sometimes hyperechoic septa can be found within the collections, and with color or power Doppler increased blood flow may be detected in the periphery [34].

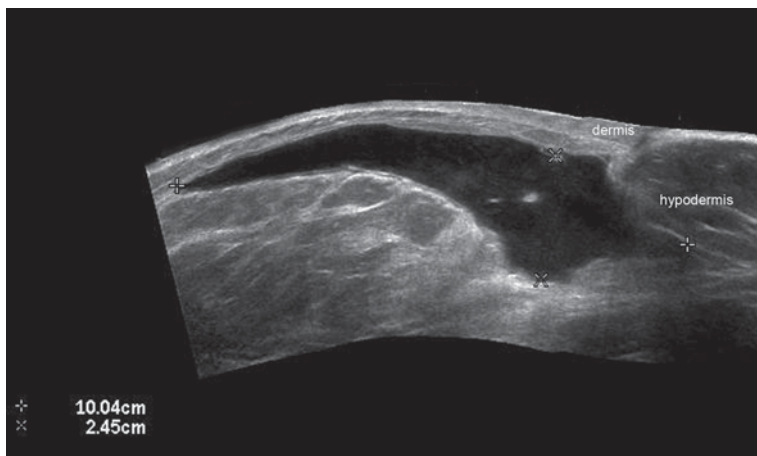


Fig. 8.12 Abscess. Ultrasound (gray scale, *transverse* view, inframammary region) shows 10.4 cm transverse \times 2.5 cm depth, anechoic fluid hypodermal collection (*between* markers) with some hyperechoic echoes due to debris

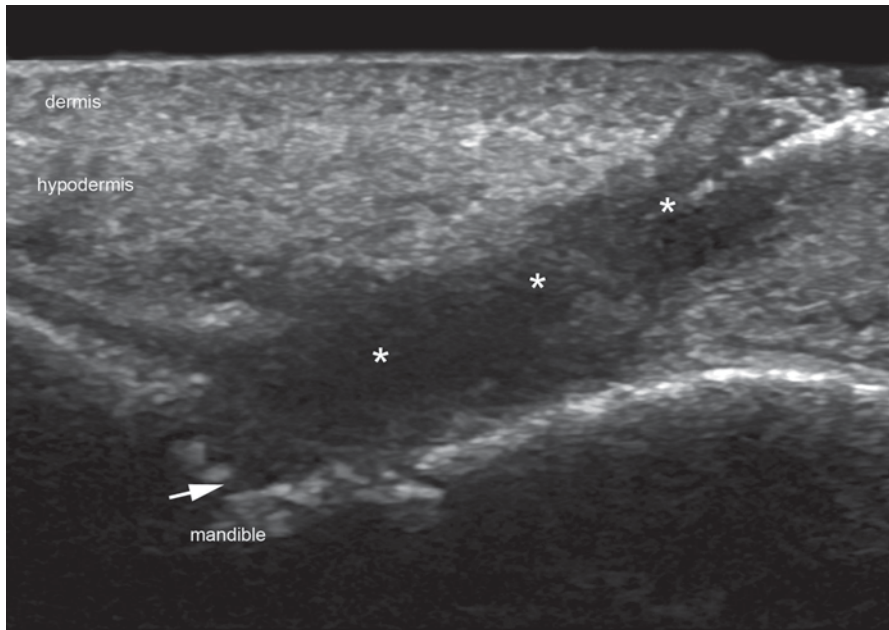


Fig. 8.13 Odontogenic fistula. Ultrasound (*gray scale, longitudinal view, chin region*) demonstrates hypoechoic fistulous tract (*) that connects the subepidermal region with the bony margin of the mandible. Notice the erosion of the bone (*arrow*) at the end of the fistula

Odontogenic Fistula

This is a dental inflammatory and infectious process that produces a fistulous connecting tract that goes from the bony margin of the maxilla or mandible to the skin. Clinically, these lesions can mimic other dermatologic diseases including malignant tumors such as basal cell carcinoma. On sonography, there is a hypoechoic or heterogeneous band connecting the bony margin of the upper maxilla or mandible with the skin. Usually an erosion of the bony margin is detected (Fig. 8.13). Hypervascularity may also be seen in the periphery of the tract [40, 43].

Warts

These are caused by infection with the human papillomavirus and commonly affect the plantar regions, although they can also be seen in the hands or other corporal locations. Clinically, they may mimic Morton's neuromas or foreign bodies. Sonographically, they appear as hypoechoic oval fusiform-shaped structures in the dermis with thickening of the epidermis. Frequently, there is hypervascularity with slow flow vessels in the dermal part of the wart which usually correlates well with

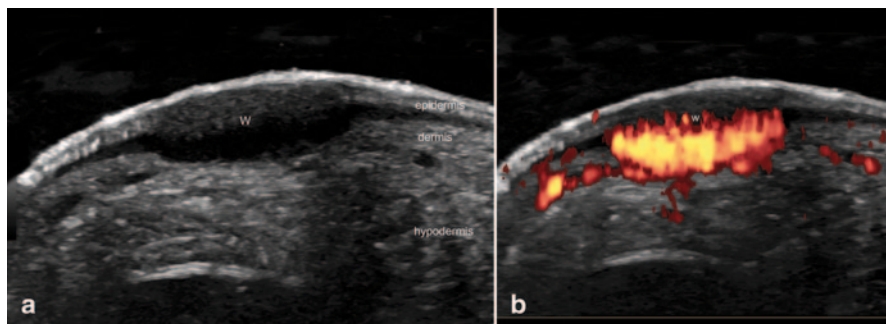


Fig. 8.14 Plantar wart (*W*). **a** Ultrasound (*gray scale, transverse view*) shows hypoechoic fusiform structure in the epidermal and dermal region. **b** Power Doppler demonstrates increased blood flow to the lesion (*in color*) in the dermis and the underlying hypodermis

the level of pain (Fig. 8.14). Thus, hypervascular warts tend to be very painful. Additionally, when the wart is located in the plantar region, commonly there is inflammation with anechoic fluid in the underlying bursa which may contribute to the patient's pain [44, 45].

Skin Cancer

This is the most frequent cancer in human beings and can be divided into nonmelanoma skin cancer (NMSC) and melanoma. NMSC can be separated into basal cell (BCC) and squamous cell carcinoma (SCC). BCC is the most frequent type and accounts for 75–80% of NMSC [46]. The use of immunosuppressive therapies for example in the recipients of renal transplants seems to be related to the increase in the prevalence of skin cancer, usually nonmelanoma type [47]. This type of cancer affects areas of the body highly exposed to the sun such as the face. Even though skin cancer shows low mortality, it can cause significant disfigurement which can be an important cosmetic problem and may decrease the quality of life of patients. Ultrasound allows the detection and measurement of the tumor in all axes. It commonly shows as a hypoechoic oval shaped lesion with hyperechoic spots. Slow flow vessels may be seen within the lesion. In tumors with a facial location, the involvement of muscle or cartilage may be detected [48, 49]. Ultrasound can also support the detection of histologic subtypes of BCC with a high risk of recurrence, such as the morpheiform, sclerosing, or micronodular forms. The latter types of BCC show a higher number of hyperechoic spots within the lesions. Thus, a cut-off point of ≥ 7 hyperechoic spots within the BCC tumor is suggestive of a high risk of recurrence histologic subtype showing a sensitivity of 79% and specificity of 53% ([50]; Fig. 8.15).

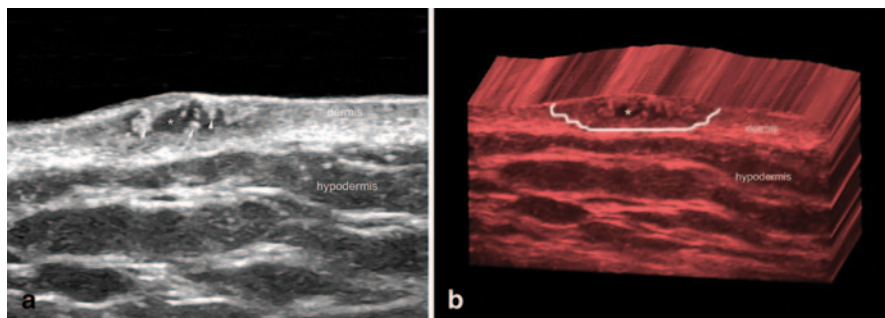


Fig. 8.15 Basal cell carcinoma of the skin (*transverse views, posterior aspect of the left shoulder*). **a** Ultrasound (*gray scale*) and **b** 3D reconstruction show hypoechoic dermal lesion (*, *outlined*) with irregular borders and hyperechoic spots (*arrows*)

Conclusion

Ultrasound is a powerful and first-line imaging tool for studying common dermatologic manifestations of rheumatologic disorders. It can provide subclinical detailed anatomical information that can be relevant for management.

References

1. Meyer J, Sans G, Rodallec C. Ultrasonics in dermatology. *Bull Soc Fr Dermatol Syphiligr.* 1951;58:266–7.
2. Alexander H, Miller DL. Determining skin thickness with pulsed ultrasound. *J Invest Dermatol.* 1979;72:17–9.
3. Murakami S, Miki Y. Human skin histology using high-resolution echography. *J Clin Ultrasound.* 1989;17:77–82.
4. El Gammal S, El Gammal C, Kaspar K, Pieck C, Altmeyer P, Vogt M, Ermert H. Sonography of the skin at 100 MHz enables in vivo visualization of stratum corneum and viable epidermis in palmar skin and psoriatic plaques. *J Invest Dermatol.* 1999;113:821–9.
5. Gropper CA, Stiller MJ, Shupack JL, Driller J, Rorke M, Lizzi F. Diagnostic high-resolution ultrasound in dermatology. *Int J Dermatol.* 1993;32:243–50.
6. Harland CC, Bamber JC, Gusterson BA, Mortimer PS. High frequency, high resolution B-scan ultrasound in the assessment of skin tumours. *Br J Dermatol.* 1993;128:525–32.
7. Seidenari S, Pagnoni A, Di Nardo A, Giannetti A. Echographic evaluation with image analysis of normal skin: variations according to age and sex. *Skin Pharmacol.* 1994;7:201–9.
8. Wortsman XC, Holm EA, Wulf HC, Jemec GB. Real-time spatial compound ultrasound imaging of skin. *Skin Res Technol.* 2004;10:23–31.
9. Wortsman X. Common applications of dermatologic sonography. *J Ultrasound Med.* 2012;31:97–111.
10. Echeverría-García B, Borbujo J, Alfageme F. The use of ultrasound imaging in dermatology. *Actas Dermosifiliogr.* 2014;pii:S0001–7310(14)00187–2. doi:10.1016/j.ad.2014.03.007.
11. Alfageme Roldán F. Ultrasound skin imaging. *Actas Dermosifiliogr.* 2014;pii:S0001–7310(14)00204-X. doi:10.1016/j.ad.2013.11.015.
12. Wortsman X. Ultrasound in dermatology: why, how, and when? *Semin Ultrasound CT MR.* 2013;34:177–95.

13. Wortsman X, Wortsman J. Clinical usefulness of variable-frequency ultrasound in localized lesions of the skin. *J Am Acad Dermatol.* 2010;62:247–56.
14. Gniadecka M. Effects of ageing on dermal echogenicity. *Skin Res Technol.* 2001;7:204–7.
15. Wortsman X, Wortsman J, Carreño L, Morales C, Sazunic I, Jemec GBE. Sonographic Anatomy of the skin, appendages and adjacent structures. In: Wortsman X, Jemec GBE, editors. *Dermatologic ultrasound with clinical and histologic correlations.* 1st edn. New York: Springer; 2013. p. 15–35.
16. Jemec GB, Serup J. Ultrasound structure of the human nail plate. *Arch Dermatol.* 1989 May;125:643–6.
17. Wortsman X, Jemec GBE. Ultrasound imaging of nails. *Dermatol Clin.* 2006;24:323–8.
18. Singh R, Bryson D, Singh HP, Jeyapalan K, Dias JJ. High-resolution ultrasonography in assessment of nail-related disorders. *Skelet Radiol.* 2012;41:1251–61.
19. Thomas L, Vaudaine M, Wortsman X, Jemec GBE, Drapé JL. Imaging the nail unit. In: Baran R, de Berker D, Holzberg M, Thomas L, editors. *Baran & Dawber's diseases of the nails and their management.* 4th edn. West Sussex: Wiley; 2012. p. 132–53.
20. Wortsman X. Sonography of the nail. In: Wortsman X, Jemec GBE, editors. *Dermatologic ultrasound with clinical and histologic correlations.* 1st edn. New York: Springer; 2013. p. 419–76.
21. Wortsman X, Wortsman J, Matsuoka L, Saavedra T, Mardones F, Saavedra D, Guerrero R, Corredoira Y. Sonography in pathologies of scalp and hair. *Br J Radiol.* 2012;85:647–55.
22. Yagyu K, Hayashi K, Chang SC. Orientation of multi-hair follicles in non baldmen: perpendicular versus parallel. *Dermatol Surg.* 2006;32:651–60.
23. Wortsman X, Wortsman J. Sonography of the scalp and hair. In: Wortsman X, Jemec GBE, editors. *Dermatologic ultrasound with clinical and histologic correlations.* 1st edn. New York: Springer; 2013. p. 477–503.
24. Seery GE. Surgical anatomy of the scalp. *Dermatol Surg.* 2002;28:581–7.
25. Wortsman X. Sonography of cutaneous and unguinal lumps and bumps. *Ultrasound Clin.* 2012. doi:10.1016/j.cult.2012.08.006.
26. Wortsman X. How to start on skin, nail and hair ultrasound: guidance and protocols. In: Wortsman X, Jemec GBE, editors. *Dermatologic ultrasound with clinical and histologic correlations.* 1st edn. New York: Springer; 2013. p. 597–607.
27. Aldrete JA. Modifications to the post anesthesia score for use in ambulatory surgery. *J Peri-anesth Nurs.* 1998;13:148–55.
28. Gutierrez M, Wortsman X, Filippucci E, De Angelis R, Filosa G, Grassi W. High-frequency sonography in the evaluation of psoriasis: nail and skin involvement. *J Ultrasound Med.* 2009;28:1569–74.
29. Gutierrez M, Filippucci E, De Angelis R, Filosa G, Kane D, Grassi W. A sonographic spectrum of psoriatic arthritis: the five targets. *Clin Rheumatol.* 2010;29:133–42.
30. Aydin SZ, Castillo-Gallego C, Ash ZR, Marzo-Ortega H, Emery P, Wakefield RJ, Wittmann M, McGonagle D. Ultrasonographic assessment of nail in psoriatic disease shows a link between onychopathy and distal interphalangeal joint extensor tendon enthesopathy. *Dermatology* 2012;225:231–5.
31. Cuoş M, Crişan M, Lenghel M, Dudea M, Croitoru R, Dudea SM. Med ultrason conventional ultrasonography and sonoelastography in the assessment of plaque psoriasis under topical corticosteroid treatment—work in progress. *Med Ultrason.* 2014;16:107–13.
32. De Agustín JJ, Moragues C, De Miguel E, Möller I, Acebes C, Naredo E, Uson J, Rejon E, Mayordomo L, Garrido J. A multicentre study on high-frequency ultrasound evaluation of the skin and joints in patients with psoriatic arthritis treated with infliximab. *Clin Exp Rheumatol.* 2012;30:879–85.
33. Gutierrez M, De Angelis R, Bernardini ML, Filippucci E, Goteri G, Brandozzi G, Lemme G, Campanati A, Grassi W, Offidani A. Clinical, power Doppler sonography and histological assessment of the psoriatic plaque: short-term monitoring in patients treated with etanercept. *Br J Dermatol.* 2011;164:33–7.

34. Wortsman X, Carreño L, Morales C. Inflammatory diseases of the skin. In: Wortsman X, Jemec GBE, editors. *Dermatologic ultrasound with clinical and histologic correlations*. 1st edn. New York: Springer; 2013. p. 73–117.
35. Sandobal C, Carbó E, Iribas J, Roverano S, Paira S. Ultrasound nail imaging on patients with psoriasis and psoriatic arthritis compared with rheumatoid arthritis and control subjects. *J Clin Rheumatol*. 2014;20:21–4.
36. Li SC, Liebling MS, Haines KA. Ultrasonography is a sensitive tool for monitoring localized scleroderma. *Rheumatology (Oxford)* 2007;46:1316–9.
37. Li SC, Liebling MS. The use of Doppler ultrasound to evaluate lesions of localized scleroderma. *Curr Rheumatol Rep*. 2009;11:205–11.
38. Wortsman X, Wortsman J, Sazunic I, Carreño L. Activity assessment in morphea using color Doppler ultrasound. *J Am Acad Dermatol*. 2011;65:942–8.
39. Wortsman X. The traces of sound: taking the road to skin. *Curr Rheumatol Rev*. 2011;7:231–8.
40. Wortsman X, Gutierrez M, Saavedra T, Honeyman J. The role of ultrasound in rheumatic skin and nail lesions: a multi-specialist approach. *Clin Rheumatol*. 2011;30:739–48.
41. Walsh M, Jacobson JA, Kim SM, Lucas DR, Morag Y, Fessell DP. Sonography of fat necrosis involving the extremity and torso with magnetic resonance imaging and histologic correlation. *J Ultrasound Med*. 2008;27:1751–7.
42. Avayú E, Rodríguez C, Wortsman X, et al. Newborn fat necrosis: case-report. *Revista Chilena Pediatría*. 2009; 80:60–4 (Spanish).
43. Cohen PR, Eliezri YD. Cutaneous odontogenic sinus simulating a basal cell carcinoma: case report and literature review. *Plast Reconstr Surg*. 1990;86:123–7.
44. Wortsman X, Sazunic I, Jemec GBE. Sonography of plantar warts: role in diagnosis and treatment. *J Ultrasound Med*. 2009;28:787–93.
45. Wortsman X, Jemec GBE, Sazunic I. Anatomical detection of inflammatory changes associated with plantar warts by ultrasound. *Dermatology* 2010;220:213–7.
46. Gniadecki R, Dam TN. Basal cell carcinoma-clinical guidelines, Danish Dermatological Society. *Forum Nord Derm Ven*. 2009;14:4–6.
47. Specchio F, Saraceno R, Chimenti S, Nistico S. Management of non-melanoma skin cancer in solid organ transplant recipients. *Int J Immunopathol Pharmacol*. 2014;27:21–4.
48. Bobadilla F, Wortsman X, Muñoz C, Segovia L, Espinoza M, Jemec GBE. Pre-surgical high resolution ultrasound of facial basal cell carcinoma: correlation with histology. *Cancer Imaging*. 2008;8:163–72.
49. Uhara H, Hayashi K, Koga H, Saida T. Multiple hypersonographic spots in basal cell carcinoma. *Dermatol Surg*. 2007;33:1215–9.
50. Wortsman X, Vergara P, Castro A, Saavedra D, Bobadilla F, Sazunic I, Zemelman V, Wortsman J. Ultrasound as predictor of histologic subtypes linked to recurrence in basal cell carcinoma of the skin. *J Eur Acad Dermatol Venereol*. 2014. doi:10.1111/jdv.12660.